Available online at www.sciencedirect.com
ScienceDirect
Journal of Molecular Catalysis A: Chemical 275 (2007) 233–239
JOURNAL OF MOLECULAR CATALYSIS A: CHEMICAL
www.elsevier.com/locate/molcata

Cross-linked poly-vinyl polymers versus polyureas as designed supports for catalytically active M^0 nanoclusters Part I. Nanometer scale structure of the polyurea support EnCat™ 40

C. Bolfa [a], A. Zoleo [a], A.S. Sassi [b], A.L. Maniero [a], D. Pears [c], K. Jerabek [d], B. Corain [a,b,*]

[a] *Dipartimento di Scienze Chimiche, Via Marzolo 1, 35131 Padova, Italy*
[b] *Istituto di Scienze e Tecnologie Molecolari, C.N.R., Sezione di Padova, Via Marzolo 1, 35131 Padova, Italy*
[c] *Reaxa Ltd., Hexagon House, Manchester M9 8ZS, UK*
[d] *Institute of Chemical Process Fundamentals, Czech Academy of Sciences, Prague-Suchdol, Czech Republic*

Received 11 December 2006; received in revised form 17 April 2007; accepted 9 June 2007
Available online 19 June 2007

Abstract

The cross-linked polymer EnCat™ 40 (polyurea) is investigated on the micro-(ESEM) and nanometer scale (ISEC, ESR, ^{13}C CP MAS NMR) both in the dry (ESEM, ^{13}C CP MAS NMR) and in the swollen state (ISEC, ESR, ^{13}C CP MAS NMR). After swelling with THF or DMF, nanoporous domains featured by ca. 1.2 nm pores are clearly detected with ISEC. ESR analysis based on the evaluation of the rotational mobility of a suitable spin probe dissolved in THF, DMF, MeOH and $PhCH_3$ as swelling media, does qualitatively confirm the presence of nanoporosity also in MeOH- and $PhCH_3$-swollen EnCat™ 40. Our manifold analysis reveals the lack of any detectable nanoporosity in water.
© 2007 Elsevier B.V. All rights reserved.

Keywords: ESR spectroscopy; Functional resins; ISEC (inverse steric exclusion chromatography); Water; THF; Nanopores

1. Introduction

The concept of cross-linked functional polymers (CFPs) as supports for metal nanoclusters employed in catalytic applications [1] dates back to 1969 [2]. The inventors of the relevant Bergbau Chemie patent claiming the one-pot synthesis of methylisobutyl ketone (MIBK) from acetone and dihydrogen recognised the potential of CFPs both for their ability to support metal nanoclusters and for providing the catalyst with specific further functionality (Scheme 1). Thus, a benchmark multifunctional catalyst capable of promoting both the acid-catalysed condensation of two acetone molecules and the hydrogenation of the resulting olefin, that turns out to be the precursor of the industrially important solvent MIBK solvent, was developed [3]. Interestingly, this concept can be further expanded (Scheme 1) to produce multifunctional catalysts bearing both diverse nanostructured metals and chemical functionalities designed for performing complex catalytic tasks.

In fact, for almost 20 years the catalysis community more or less neglected this concept, which was only described in the above referenced German patent [2]. However, by the mid-1990s a systematic exploration of the field was started in these laboratories and by other workers [1,4,5].

The CFPs employed before the advent of the EnCat™ support have been generally classic co-poly-vinylolefin-diolefin materials both macroreticular and gel-type in nature [6,7].

Early this decade (see for example [8–10]) Ley and associates proposed a somewhat unusual support for both nanostructured Pd^0 and "ionic" Pd^{II} (*vide infra*), being a functional gel-type cross-linked homo-polymer resulting from the interfacial polymerisation of aryl poly-functional isocyanates dissolved in organic solvent and suspended in water (Fig. 1), and later trademarked as EnCat™ by Reaxa Ltd. The resin soon became the basis for a number of supported Pd^{II} complexes and Pd^0 nanocomposites available commercially under the EnCat™ trademark.

* Corresponding author at: Dipartimento di Scienze Chimiche, Via Marzolo 1, 35131 Padova, Italy.
E-mail address: benedetto.corain@unipd.it (B. Corain).

1381-1169/$ – see front matter © 2007 Elsevier B.V. All rights reserved.
doi:10.1016/j.molcata.2007.06.011

$M^0/Ⓟ\text{-}F_i$

M^0 = nanostructured metal centre Ⓟ = CFP ($F_i = F_1, F_2, \ldots, F_n$)

Scheme 1. The concept of poly-functionality of a nanocomposite obtained from a nanostructured metal (0) and a cross-linked functional polymer.

1.1. The "primary structure" of EnCat™

A general scheme aimed at the illustration of the transformation of a poly-phenylisocyanate into a cross-linked functional polymer, a polyurea, is depicted in Fig. 1.

It is seen that a given fraction of the initial –NCO groups undergo a controlled hydrolysis to give $–NH_2$ groups, which immediately react with remaining –NCO groups to form a cross-linked polymer framework.

We report in this paper on a thorough micro- and nanometer scale characterisation of this promising catalyst support matrix using a broad spectrum of techniques including: ESEM (environmental scanning electron microscopy), ESR (electron spin resonance), MAS NMR (magic angle spinning nuclear magnetic resonance) and ISEC (inverse steric exclusion chromatography).

2. Experimental

Solvents were of reagent grade and were used as received. EnCat™ 40 was obtained from Reaxa Ltd. and it was used as received. TEMPONE (2,2,6,6-tetramethyl-4-oxo-1-oxypiperidine) was a commercial product received from Sigma–Aldrich and was also used as received. Details on ISEC apparatus and on the preparation of samples to be examined with ISEC and ESR are given elsewhere [11a].

ESEM analysis was carried out with an ESEM Philips XL 30 apparatus and the resin was analyzed both in the dry and in the swollen (DMF) state.

ESR spectra were collected with an Elexsys Bruker spectrometer at 290 K, after 10 scans; excitation frequency was 9.68 GHz with 100 KHz modulation. Microwave power and modulation amplitude (typically 0.2 mW and 0.1G, respectively) were carefully chosen in order to avoid saturation and line shape distortion.

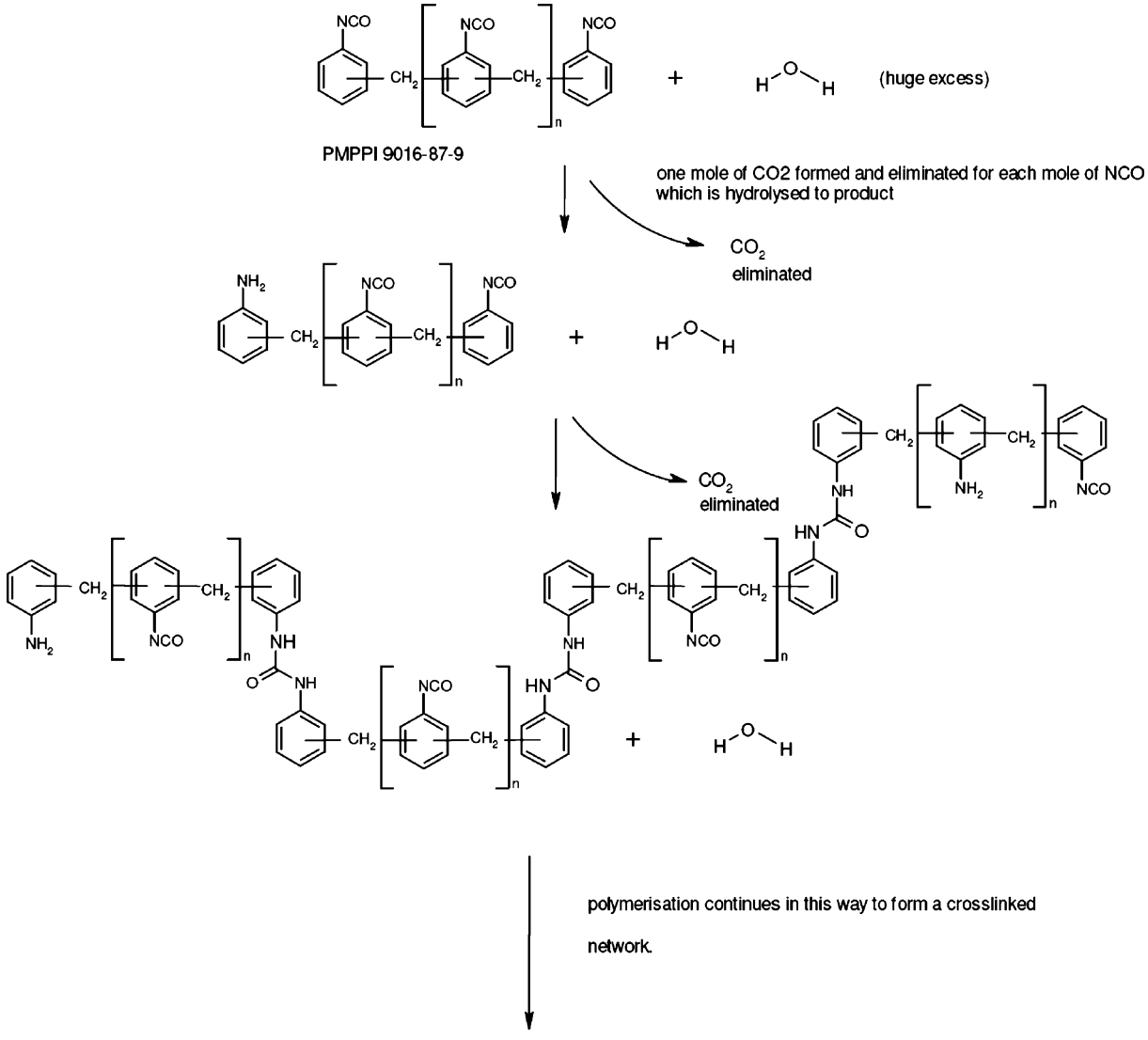

Fig. 1. Scheme of the transformation of a polyisocyanate into a cross-linked polyurea polymer by controlled partial hydrolysis of isocyanate groups.

The 50.26 MHz ^{13}C CP (cross-polarization) MAS NMR spectra were collected on a Bruker AC 200 spectrometer equipped for solid-state analysis. Samples were spun at 3300 Hz in 7 mm diameter zirconia rotors, with Kel-F® cap and sealed with Teflon o-ring. ^{13}C chemical shifts were externally referenced to solid sodium 3-(trimethyl-silyl)-1-propane sulfonate at 0 ppm. Cross-polarization experiments were optimized using adamantane. Magic angle conditions were adjusted by observing ^{79}Br spinning side bands pattern in a rotor containing 5% of KBr. All spectra were obtained using the standard Bruker cross-polarization (CP) pulse sequence, with high power proton decoupling during acquisition, 7 s relaxing delay, and processed with a 10 Hz exponential line broadening.

The CP technique has been developed to increase the signal to noise ratio in rare spin spectra (e.g. ^{13}C NMR spectra) through magnetization transfer from a second abundant spin system (e.g. ^{1}H). The key parameter of the CP pulse sequence is the contact time (CT), i.e. the period (ms) during which the magnetization transfer takes place. For a given chemical functionality, the overall rate of the magnetization transfer process is related to the molecular dynamic of the observed fragment: the slower is the motion, the faster is the magnetization transfer and the higher is the relative intensity of the NMR signal. For this reason, the solid-state ^{13}C NMR measurements obtained through cross-polarization cannot be readily exploited for quantitative analysis. For the same reason, the CP spectra of a given polymer collected with different contact times generally show a different relative intensities pattern. It is also noteworthy that the signal arising from highly mobile moieties displays a lower peak-width with respect to slowly moving segment of polymer, mainly due to the dipolar interactions averaging. As a matter of fact, when variable contact time measurements are employed to study polymers in the swollen state, one can expect that CT increasing will enhance the signal arising from highly mobile fragments of the polymer, i.e. the part of the matrix that is in full contact with the solvent [11a], which is characterized by smaller peak-width.

3. Results

In this study we have employed ESEM, ESR, CP MAS NMR and ISEC in an integrated fashion [11]. The usefulness of a multi-method strategy to characterise the exact nanostructural features of gel-type CFP in their working state has been illustrated by us in a number of cases [11]. To this end, in this work we employ a combination of ISEC, CP MAS NMR and ESR, which provide independent information (*vide infra*) on the nanometer scale porosity of the matrix in a liquid medium. ISEC enables the quantitative evaluation of the nanometric empty spaces featuring the swollen polymer framework in that medium, CP MAS NMR provides an estimate of the degree of interaction of the polymer chains with that medium and ESR permits a fine measurement of the rotational mobility of a given paramagnetic steric probe inside the liquid-filled nanopores. As we have previously reported [11b,d], the rotational correlation time of the TEMPONE probe does quantitatively correlate with the nanoporosity of the swollen material, the ESR datum becomes an independent tool relevant to the nanometer scale porosity of the examined material.

3.1. The micrometer scale structure of EnCat™ 40

For micrometer scale investigation we utilised ESEM (i.e. environmental scanning electron microscopy), a modern version of SEM that makes possible the examination of samples without the necessity of any pre-treatment with graphite or gold. One of the attractions of this technique is that it allows sample evaluation in the presence of significant amounts of a liquid medium providing its boiling point is not too low. Dimethyl formamide (DMF) fulfils this requirement and is known as a good swelling medium for the EnCat™-matrix. The EnCat™ 40 was supplied as 50–300 μm beads, the microstructure of which is illustrated in Fig. 2a–f.

The external surface of the polyurea beads (Fig. 2a) exhibits an unusual roughness, which suggests the likely major feature of the internal microstructure. In fact, the section of a broken bead reveals that EnCat™ 40 particles consist of an array of tightly bound, very compact sub-particles (Fig. 2c and f) both in the dry and swollen state (Fig. 2c and f). Inspection of Fig. 2a–f reveals conclusively that EnCat™ 40 beads are not true microcapsules with a traditional hollow core and shell morphology. Thus, it could be argued that it is somewhat misleading to refer to these catalysts as microencapsulated homogeneously.

3.2. The nanometer scale structure of EnCat™ 40

An understanding of the nanometer porosity of CFPs in 'good' solvents able to swell the matrix is important in order to be able to understand the properties of the matrix as a catalyst support. This crucial feature of the support itself can be successfully investigated with ISEC (inverse steric exclusion chromatography) based on analysis of elution behaviour of standard solutes on a column filled with the polymer matrix under investigation [12–14]. Using this chromatographic technique the porosity of palladium-containing materials Pd^{II} EnCat™ 30 and Pd^{II} EnCat™ 40 swollen in THF have already been investigated [15]. In Pd^{II} EnCat™ 30 pores were found with diameter 1.2 nm and volume 1.6 cm^3/g and in Pd^{II} EnCat™ 40 pores with diameter 0.7 nm and volume 0.7 cm^3/g. Note that the two materials are in fact macromolecular Pd^{II} complexes containing ca. 4.5% metal and their nanostructure could be appreciably affected by the presence of Pd^{II}. The texture information was obtained from chromatographic data using commercial POROCheck™ software program (POROCheck™ software is available from Polymer Standards Service GmbH, website www.polymer.de) based on Gorbunov et al.'s approach [16] developed mainly for the characterization of chromatography column media by considering symmetrical smooth pore size distribution characterized by pore volume, medium pore diameter and the distribution width only. In this study we employed an alternative method, more suitable for assessment of the morphology of functional polymers having a less regular morphology [13–15]. The technique is based on the idea of representing the real pore structure with a set of discrete pore fractions of simple

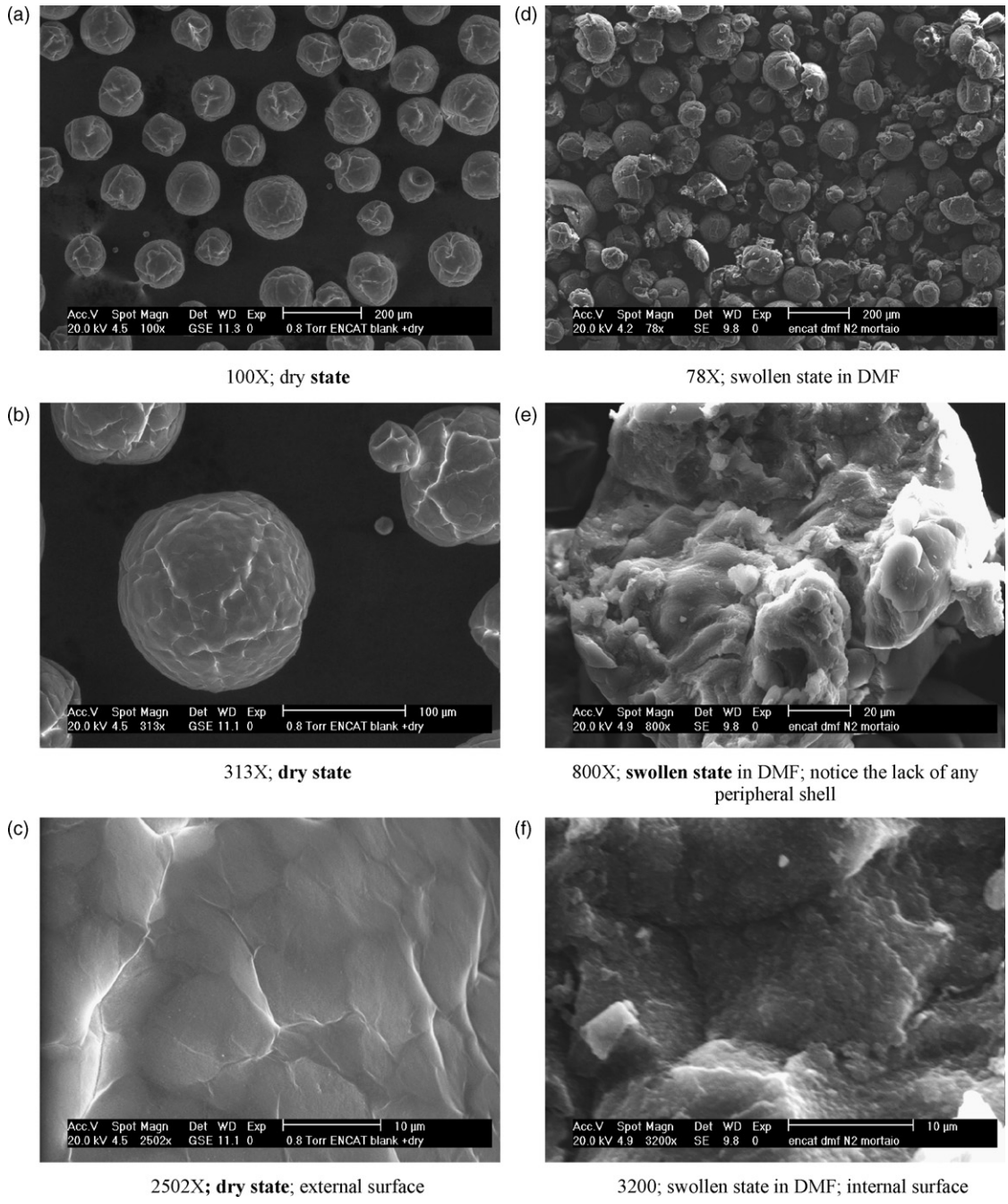

Fig. 2. (a–f) SEM images of EnCat^{TM} 40 in the dry (a–c) and DMF-swollen (d–f) state.

geometrical shape. Characteristic dimensions of these fractions are set beforehand as a scale by which the examined material is assessed and the mathematical treatment of the experimental chromatographic data then produces volumes of the individual model pore fractions [13].

Results of our evaluation of the swollen state morphology of EnCat^{TM} 40 in terms of the conventional cylindrical pore model are shown in Fig. 3. From these results computed volume-averaged pore diameter is 1.2 nm and total pore volume 1.5 cm^3/g.

Results illustrated in Fig. 3 are in agreement with the pore sizes reported in Ref. [15] for Pd^{II} EnCat^{TM} 40. Comparison of the pore volumes with the true volume of the examined samples determined from the difference between the known volume of the empty column and the elution volume of totally excluded solute reveals that the estimated volumes of the cylindrical pores are too big and do not leave enough space for the solid part of the examined materials. From our experiences with swollen polymer morphology characterization, we know that the quantitative part of the polymer morphology description – the pore volume – can be systematically overestimated [14]. In many studies [14] we found that a useful simplified geometrical representation of the morphology of swollen polymers can be devised using the model proposed by Ogston [17], in which the pores are spaces

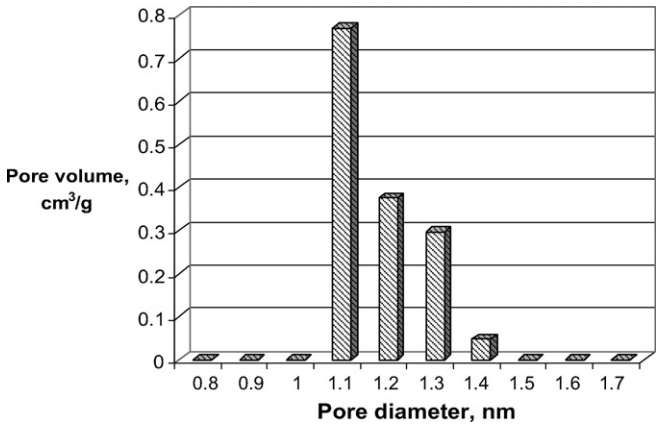

Fig. 3. Pore size distribution for EnCat™ 40 support in the THF-swollen state as evaluated from ISEC data using modelling of the texture as a set of discrete fractions of cylindrical pores.

between randomly oriented cylindrical rods. In this model the pore dimension parameter is concentration of the cylindrical rods in units of length per unit of volume [nm/nm^3 = nm^{-2}], i.e. the so-called polymer chain concentration. It is important that the volume determined for this model is the volume of the whole system and not the volume of the pores only. An auxiliary parameter of Ogston's model is the diameter of the cylindrical rods. It is a constant that influences the overall volume of the model system but it practically does not influence the fitting of experimental data. For EnCat™ 40 materials we chose 0.2 nm as the size of this parameter. The morphology of the polymer, evaluated with Ogston's model, is shown in Table 1.

It is important that the volume determined for the Ogston's model is the volume of the whole system and not the volume of the pores only. In an ideal case, the sum of the volumes of the model fractions (ΣV_i) should be equal to the true volume of the swollen polymer ($V_{\text{tot gel}}$), which can be determined with good precision from the difference between known volume of the empty column and the elution volume of totally excluded solute.

In water ISEC detected no porosity and the $V_{\text{tot gel}}$ determined is close to the volume expected for an unswollen polymer. In the organic solvents the model volume ΣV_i is close to the true swollen polymer volume only for the THF-swollen matrix. In the other solvents the calculated model volume is smaller than the true one and this suggests some of the polymer domains are too dense to be "visible" to the chromatographic examination technique. The difference was particularly large in the toluene-swollen matrix.

EnCat™ 40 exhibits a fairly homogeneous morphology similar to that of a classic highly cross-linked gel-type functional copolymer [13,14]. There was no evidence for wider pores, which might have been anticipated from a reticulation or phase separation mechanisms during polymerization. Certain roughness of the internal surface revealed in ESEM pictures of swollen EnCat™ 40 (Fig. 2f) suggests probable reticulation on a micrometer scale. Presence of resulting "super macroporosity" could not be revealed by ISEC, which cannot detect pores wider than about 100 nm. Such pores could facilitate transport between bulk phase and the interior of the particles but their capacity to support functionality would be insignificant. Practically all the supported functionality must be located in the narrow pores of the polymer network and its accessibility must strongly depend on the swelling of the polymer in an appropriate solvent. The polyurea backbone of the EnCat™ materials swells reasonably well in organic solvents but in aqueous environment the supported catalytic centers would be inaccessible.

In conclusion the ISEC data would suggest that water is a poor solvent of choice as a viable reaction medium in that neither meso- nor nanopores appear to be developed by swelling. In contrast, toluene (TOL), tetrahydrofurane (THF) and dimethylformamide (DMF) turn out to be reasonable swelling media. In these solvents, nanopores near to 1 nm in diameter appear to be dominant. This value is significant and supported by the ESR results presented in Section 3.3 that deal with a spin (and steric) probe whose hydrodynamic radius is ca. 0.3 nm.

3.3. Molecular accessibility of the swollen nanoporous domains of EnCat™ 40 to molecules of substantial size: ESR and ^{13}C MAS NMR evaluations

ESR has been known for decades [18] as a powerful tool for the quantitative evaluation of the rotational dynamics of spin probes of well-defined sizes. In fact, this technique provides information on both the ability of a given molecule for gaining access to the nanoporous domains of a hosting material and

Table 1
Nanometer scale morphology of EnCat™ 40 in THF as shown by Ogston's model for the chain diameter equal to 0.2 nm

	Polymer fraction volume (cm^3/g)			
	THF	Toluene	DMF	Water
Polymer chain concentration (nm/nm^3)				
0.1	0	0	0	0
0.2	0	0	0	0
0.4	0	0	0	0
0.8	0	0	0	0
1.5	0.14	0	0.49	0
3	1.29	0.89	1.19	0
Cummulative model volume, ΣV_i (cm^3/g)	1.43	0.89	1.68	0
True swollen polymer volume, $V_{\text{tot gel}}$ (cm^3/g)	1.48	1.84	2.10	1.04

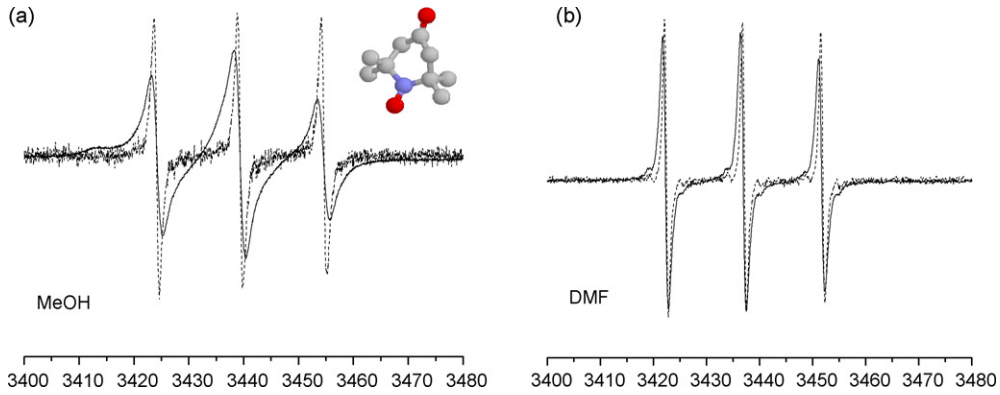

Fig. 4. ESR spectra of TEMPONE (molecular sketch in (a)) in EnCat^{TM} 40 after swelling in methanol (a) and in dimethylformamide (b). Dotted line: TEMPONE in bulk; solid line: TEMPONE in EnCat^{TM} 40.

also its freedom for rotation within the pores. In this context, it should be emphasised that the ability of TEMPONE to move in the interior of EnCat^{TM} 40 provides a valuable assessment of steric conditions relevant for a myriad of potential reagents to be employed in catalytic work based on this support matrix. Two representative ESR spectra are shown in Fig. 4.

Analysis of the spectra reveals that the spin probe undergoes a unique motion regime in each accessible nanopore [18]. There was no indication of nanodomains in which the TEMPONE rotation either strongly slowed down or even hindered in anyway [18], in any of the tested liquid media. In fact, the occurrence of this situation would produce a spectral pattern well documented in Ref. [18], quite in contrast with the present findings.

Information on rotational mobility extracted from ESR spectra (determined as in Ref. [11a]) is presented in Table 2. The rotational mobility of TEMPONE undergoes a marked decrease (higher τ values) in all media except for water. However, as revealed by the ISEC results, EnCat^{TM} 40 does not swell in water and the ESR signal in this instance is due to TEMPONE present in occluded solution rather than to molecules located inside polymer nanocavities. The effect of the polymer environment on the rotational mobility is particularly strong in methanol ($\tau = 627$ ps) where, owing to lower swelling, the steric conditions are particularly constrained. In TOL, DMF and THF, TEMPONE readily gains access to the nanopores of EnCat^{TM} 40. In these media, rotation is relatively unhindered [18] and only moderately slower than in the bulk media. A useful numerical expression of the effect of the polymer matrix on the mobility of molecules inside the polymer cavities seems to be $\ln(\tau/\tau_0)$

Table 2
Rotational mobility of TEMPONE in various swelling media confined inside EnCat^{TM} 40, measured at 290 K

Solvent	τ (ps)[a]	τ_0 (ps)[b]	$Y = \ln(\tau/\tau_0)$
H_2O	16.6	17.0	–
MeOH	627	17.3	3.6
$PhCH_3$	59.6	5.2	2.4
DMF	77.5	12.0	1.9
THF	49.0	7.9	1.8

[a] Rotational correlation time of TEMPONE inside the swollen nanoporous domains EnCat^{TM} 40.
[b] Correlation time in unconfined solvents.

Table 3
^{13}C MAS NMR data of EnCat^{TM} 40 in the dry state and after swelling in water and DMF for three different contact times (CT, ms)

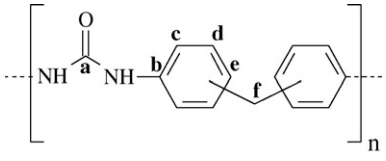

Sample state	**a**		**b** and **e**		**d**		**c**		**f**	
	δ (ppm)	$W_{1/2}$ (Hz)	δ (ppm)	$W_{1/2}$ (Hz)	δ (ppm)	$W_{1/2}$ (Hz)	δ (ppm)	$W_{1/2}$ (Hz)	δ (ppm)	$W_{1/2}$ (Hz)
Dry CT = 1	155.4	365	136.1	468	128.6	317	120.0	450	38.4	543
Dry CT = 3	154.8	360	135.9	458	128.4	300	120.1	439	38.7	474
Dry CT = 5	154.7	336	135.9	428	128.5	320	119.9	465	38.3	469
H_2O CT = 1	155.2	331	136.0	453	128.5	331	119.8	401	39.7	367
H_2O CT = 3	155.4	320	136.1	421	128.6	300	119.6	401	39.4	306
H_2O CT = 5	154.9	320	135.9	420	128.5	296	119.8	400	39.5	407
DMF CT = 1	154.1	218	136.3	413	129.1	258	119.2	282	39.3	472
DMF CT = 3	153.9	214	136.2	346	128.8	256	118.9	276	–	–
DMF CT = 5	154.1	130	136.5	318	129.2	237	118.9	254	–	–

(Table 2). This quantity reveals a trend of solvent compatibility that may be useful in the practical application of catalysts based on the EnCat^{TM} 40 matrix.

^{13}C CP MAS NMR is also a useful analytical tool for evaluating, at the nanometer scale, the ability of a given liquid medium to permeate a suitable swellable material. When applied to the investigation of a cross-linked functional polymer in the dry and in the swollen state [11], we observe that the most powerful exploitation of ^{13}C CP MAS NMR is achieved when a suitable pendant arm containing two to four carbon atoms hangs from the polymer backbone. In that case, the side arm behaves as a sensitive probe for detecting the relative degree of "solid state" or of "swollen state" of the polymer framework [11]. In this case the situation is more difficult in that there is no convenient pendant arm and so the analysis has to focus on the CH_2 and the aromatic carbon atoms.

In particular, we have to concentrate on the line width of the relevant signals as a function of the contact time, CT (Table 3).

In the presence of water, the line width at half maximum $W_{1/2}$ of aromatic carbons and of methylene groups bands in the solid state turn out to be substantially unaffected by the interaction of EnCat^{TM} 40 with the swelling medium. In DMF, $W_{1/2}$ decreases for all relevant bands at all employed CTs and it is seen to decrease with the increase of CT. This observation supports the co-presence of domains featured by different degrees of swelling, in the polymer framework. However, in MeOH, TOL and THF the pattern is far more complex, without any detectable trend in the effect of CT on the various resonance bands.

Although the ^{13}C MAS NMR data are limited they support the picture provided by the ISEC and ESR analyses.

4. Conclusions

EnCat^{TM} 40 is a gel-type cross-linked functional polymer that in the dry state lacks any porosity. ESEM investigation on the DMF-swollen matrix suggests that the polymer particles are not completely glassy but possess certain microstructure, which is revealed after swelling. However, even though these macrostructures could contain in fact macropores after complete swelling ("invisible" to ISEC), we can safely state that the polymer framework is mainly built up with nanopores (ISEC evidence, Table 1). Evidently, the "working arena" for any catalytic center supported on this carrier matrix are nanocavities within the polymer gel fully dependent on swelling. The density of the polyurea matrix of the EnCat^{TM} 40 as depicted by ISEC is rather high and even in good swelling media like THF or DMF the openings in the network have effective size around 1.2 nm. As indicated by ESR spectroscopy, cavities of this size significantly influence mobility of hosted molecules. In less effective swelling solvents like toluene or methanol, the accessibility of the support interior to substrates appears to be limited and in an aqueous environment there is no accessibility to the TEMPONE probe.

References

[1] B. Corain, P. Centomo, S. Lora, M. Kralik, J. Mol. Catal. A: Chem. 204–205 (2003) 755.
[2] J. Wöllner, W. Neier, German Patent 1260454 (1969).
[3] R. Wagner, P.M. Lange, Erdöl Erdgas Kohle 105 (1989) 414.
[4] B. Corain, M. Kralik, J. Mol. Catal. A: Chem. 159 (2000) 153.
[5] B. Corain, M. Kralik, J. Mol. Catal. A: Chem. 173 (2001) 99, and its corrigendum J. Mol. Catal. A: Chem. 200 (2003) 333.
[6] A. Guyot, in: D.C. Sherrington, P. Hodge (Eds.), Synthesis and Separations using Functional Polymers, Wiley, New York, 1988.
[7] B. Corain, M. Zecca, K. Jerabek, J. Mol. Catal. A: Chem. 177 (2001) 3.
[8] C. Ramarao, S.V. Ley, S.C. Smith, I.M. Shirley, N. DeAlmeida, Chem. Commun. (2002) 1132.
[9] J.-Q. Yu, H.-C. Wu, C. Ramarao, J.B. Spencer, S.V. Ley, Chem. Commun. (2003) 678.
[10] S.V. Ley, C. Mitchell, D. Pears, C. Ramarao, J.-Q. Yu, W. Zhou, Org. Lett. (2003) 4665.
[11] (a) F. Pozzar, A. Sassi, G. Pace, S. Lora, A.A. D'Archivio, K. Jerabek, A. Grassi, B. Corain, Chem. Eur. J. 11 (2005) 7395;
(b) A. Biffis, B. Corain, M. Zecca, C. Corvaja, K. Jerabek, J. Am. Chem. Soc. 117 (1995) 1603–1606;
(c) M. Zecca, A. Biffis, G. Palma, C. Corvaja, S. Lora, K. Jerabek, B. Corain, Macromolecules 29 (1996) 4655–4661;
(d) A.A. D'Archivio, L. Galantini, A. Panatta, E. Tettamanti, B. Corain, J. Phys. Chem. B 102 (1998) 6774–6779.
[12] K. Jerábek, Anal. Chem. 57 (1985) 1595.
[13] K. Jerábek, Anal. Chem. 57 (1985) 1598.
[14] K. Jerabek, Cross evaluation of strategies in size-exclusion chromatography, in: M. Potschka, P. LDubin (Eds.), ACS Symposium Series, vol. 635, American Chemical Society, Washington, DC, USA, 1996, pp. 211–224.
[15] D.A. Pears, S.C. Smith, Aldrichim. Acta 38 (2005) 23.
[16] A.A. Gorbunov, L.Y. Solovyova, V.A. Pasechnik, J. Chromatogr. 448 (1988) 307.
[17] A.G. Ogston, Trans. Faraday Soc. 54 (1958) 1754.
[18] P.L. Nordio, in: L.J. Berliner (Ed.), Spin Labeling, Theory and Applications, vol. I, Academic Press, New York, 1976, pp. 5–52.